Propagation of Dark Stripe Beams in Nonlinear Media: Snake Instability and Creation of Optical Vortices

A. V. Mamaev* and M. Saffman
Department of Optics and Fluid Dynamics, Risø National Laboratory, Postbox 49, DK-4000 Roskilde, Denmark

A. A. Zozulya
Joint Institute for Laboratory Astrophysics, University of Colorado, C.B. 440, Boulder, Colorado 80309-0440
(Received 27 November 1995)

We analyze the evolution of (1+1) dimensional dark stripe beams in bulk media with a photorefractive nonlinear response. These beams, including solitary wave solutions, are shown to be unstable with respect to symmetry breaking and formation of structure along the initially homogeneous coordinate. Experimental results show the complete sequence of events starting from self-focusing of the stripe, its bending due to the snake instability, and subsequent decay into a set of optical vortices.

PACS numbers: 42.65.Jx, 42.65.Hw, 42.65.Tg

Focusing Kerr-type nonlinear media exhibit solitary wave solutions, where diffraction is compensated by the nonlinearity. These solutions are localized bright beams with zero field at infinity. Solitary solutions in defocusing media correspond to a dark region of small intensity with finite (and larger) intensity at infinity. Stripe (1+1) dark solitary solutions of the nonlinear Schrodinger equation in the context of a defocusing Kerr nonlinearity were analyzed in Ref. [1]. Later it became evident that these solutions are unstable in bulk media [2,3] due to the growth of perturbations along the initially homogeneous coordinate. Their breakup and subsequent spatial dynamics have been the subject of continuing interest since then [4]. Numerical analysis of spatial dynamics of light beams for a nonsaturable and saturable defocusing Kerr nonlinearity was undertaken in [5] and [6], respectively.

Dark solitary wave solutions can only be investigated in approximate form experimentally, since they have finite energy at infinity. Experimental investigations of the propagation of dark stripe beams in bulk media have relied, therefore, on embedding a dark notch in a somewhat wider bright envelope [7–11]. This has two immediate consequences. First, the bright envelope spreads in a defocusing medium, which limits the propagation distance over which a high contrast dark stripe can be maintained. Second, the growth rates for perturbations along the homogeneous coordinate turn out to depend on the relative width of the envelope to the dark notch. We have found, both theoretically and experimentally, that the instability growth rates decrease as the envelope of the bright background is narrowed. This may in part explain why the snake instability of dark stripe beams, observed here for the first time, has not been reported previously.

We analyze below the breakup and subsequent spatial evolution of one-transverse-dimensional (1+1) dark stripe beams in bulk nonlinear media with a photorefractive nonlinear response. In bulk media these beams belong to a low-dimensional (1+1) subclass of higher-dimensional (2+1) allowable solutions and are shown to be unstable due to breaking of the initially odd symmetry of the field and the appearance of spatial structure along the "hidden" homogeneous coordinate. We present theoretical and experimental data demonstrating all stages of this breakup and subsequent spatial evolution resulting in the formation of optical vortices (wave front dislocations) [12]. Formation of optical vortices has been predicted in laser cavities [13], and due to nonlinear propagation , in self-defocusing media [6,14]. Optical vortices are well known in linear optics [15], and were observed previously in self-defocusing optical media [9] by introducing strong perturbations at the entrance to the nonlinear medium. We demonstrate here that optical vortices are a natural consequence of nonlinear propagation of any dark stripe beam in a defocusing medium. The necessary seeds are provided by the natural noise in the system, and the characteristic scales are determined by the fastest-growing modes of the transverse modulation instability.

Propagation of an optical beam $B(\vec{r})$ in a defocusing photorefractive medium is governed by the equations [16]

$$\left[\frac{\partial}{\partial x} - \frac{i}{2}\nabla^2\right]B(\vec{r}) = -i\,\frac{\partial\varphi}{\partial z}B(\vec{r}), \tag{1a}$$

$$\nabla^2\varphi + \nabla\ln(1+|B|^2)\cdot\nabla\varphi = \frac{\partial}{\partial z}\ln(1+|B|^2). \tag{1b}$$

where φ is the electrostatic potential induced by the beam with the boundary conditions $\nabla\varphi(\vec{r}\to\infty)\to 0$. Equations (1a) and (1b) imply a particular geometry of interaction where a beam propagates along one of the crystal axes (the x axis) and the electrooptic tensor has one dominating component, e.g., as is the case for a photorefractive crystal of SBN. The differential operator ∇ acts on coordinates y and z perpendicular to the direction of propagation of the beam x. The relationship between the dimensionless coordinates (x, y, z) and the physical coordinates (x', y', z') is given by the expressions $x = |\alpha|x'$ and $(y, z) = \sqrt{k|\alpha|}\,(y', z')$, where $\alpha = (1/2)kn^2r_{33}(E_{\rm ext} + E_{\rm ph}) < 0$. Here k is the wave

 0031-9007/96/76(13)/2262(4)$10.00 © 1996 The American Physical Society

number of electromagnetic radiation in the medium, n is the index of refraction, r_{33} is the relevant component of the electro-optic tensor, $E_{\rm ph}$ is the amplitude of the photogalvanic field, and $E_{\rm ext}$ is the amplitude of the external field far from the beam; both are directed along the z coordinate. The electromagnetic intensity $|B(\vec{r})|^2$ is normalized to the dark intensity I_d.

If all functions in Eqs. (1) are assumed to depend only on the transverse coordinate z, the photorefractive nonlinearity becomes identical to the saturable Kerr nonlinearity. Equation (1b) can be integrated and Eq. (1a) recast in the form

$$\left[\frac{\partial}{\partial x} - \frac{i}{2}\frac{\partial^2}{\partial z^2}\right]B(x,z) = -i\,\frac{|B|^2 - |B_\infty|^2}{1 + |B|^2}\,B\,, \qquad (2)$$

where $|B_\infty| = |B(z = \pm\infty)|$. The simplest solitary wave solution of Eq. (2) has the form $B(x,z) = b(z)$ with $b(z)$ governed by the relation [17]

$$db/dz = \sqrt{2}\sqrt{c - c_m - c_m \ln c/c_m}\,, \qquad (3)$$

where $c = 1 + b^2$, $c_m = 1 + b_m^2$, $b_m = b(\infty) = -b(-\infty)$. This antisymmetric solution is analogous to that obtained by Zakharov and Shabat in Ref. [1] for nonsaturable Kerr nonlinearity and reduces to it in the limit $b_m \ll 1$. The question of stability of this solution with respect to transverse modulation is addressed by considering the amplitude of an electromagnetic field of the form $B(\vec{r}) = [b(z) + \delta b(z)\,\exp(\Gamma x)\,\sin(k_y y)]$, where $b(z)$ is the solution (3), k_y is an arbitrary transverse wave number, δb is a small complex-valued perturbation eigenmode, and Γ is the growth rate of this eigenmode.

The system of equations for the eigenmodes obtained by linearization of Eqs. (1) is of the form

$$\left[\Gamma + \frac{b^2 - b_m^2}{1 + b^2} + \frac{1}{2}k_y^2 - \frac{1}{2}\frac{\partial^2}{\partial z^2}\right]\delta b = -b\,\delta\varphi\,, \qquad (4a)$$

$$\frac{\partial^2}{\partial z^2}\,\delta\varphi - k_y^2\delta\varphi + \frac{\partial}{\partial z}\left[\delta\varphi\,\frac{\partial}{\partial z}\,\ln(1 + b^2) - \frac{1 + b_m^2}{1 + b^2}\,\frac{\partial}{\partial z}\,\frac{b(\delta b + \delta b^*)}{(1 + b^2)}\right] = 0\,. \qquad (4b)$$

The eigenvalues Γ may be either purely real or purely imaginary. Real positive values of Γ correspond to growing modes and to the instability of the ground state. Figure 1 shows the numerically found instability growth rate Γ for the solution (3) as a function of the transverse wave number k_y and for two values of its maximum intensity $I_m = b^2(z = \pm\infty)$. Figure 1 demonstrates that the solution (3) is unstable in a certain range of transverse wave numbers k_y. The eigenmodes turn out to be even functions of the coordinate z, whereas the ground state solution (3) is odd. Because of this difference in parities, growth of the perturbation eigenmode causes the initially straight dark stripe (3) to bend periodically along the y axis. That is why this instability is also called snake instability [2].

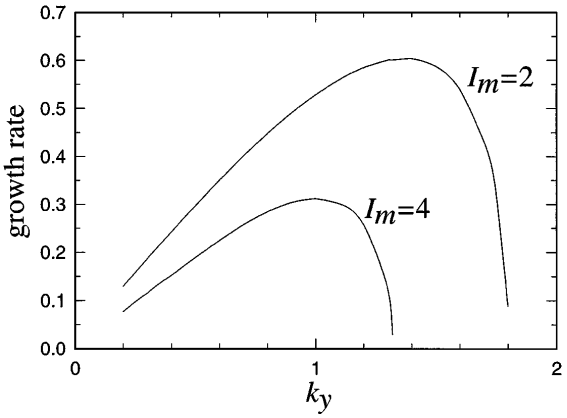

FIG. 1. Modulation instability growth rate Γ as a function of the transverse wave number k_y for the dark solitary wave solution (3).

To study the nonlinear stage of spatial dynamics Eqs. (1) have been solved numerically for several different input field profiles including the solitary solution (3). The results presented below correspond to our experiments where the dark intensity notch was imbedded in a large-diameter bright stripe beam. The input electromagnetic field in this case was chosen to be of the form $B_{\rm in} = B_0(z)[1 + B_N(y,z)] \equiv B_0(z) + N(y,z)$, where B_0 is a (1+1) ground state and B_N is an additive noise with uniform random spectrum in Fourier space. The relative magnitude of noise is characterized by the parameter $\epsilon = \int |N|^2 dy dz / \int |B_0|^2 dy dz$, where the integration is carried out over the computation window.

The ground state has the form

$$B_0(z) = \sqrt{I_m}\,\exp[-4z^2/d^2 + \pi i\theta(z)]\Phi(z)\,, \qquad (5)$$

where $\Phi(z) = 1 - \exp(-400z^2/d^2)$, I_m is the initial intensity of the beam, and $\theta(z)$ is the step function $\theta(z > 0) = 1$ and $\theta(z < 0) = 0$. The electromagnetic field (5) is a wide beam with a Gaussian intensity profile and the diameter d having a dark notch in the center with 10 times smaller diameter. The relative phase of the left and right halves of the beam is shifted by 180° so that the field passes through zero at the center and changes sign.

Figure 2 demonstrates the spatial dynamics of the beam (5) with $d = 60$, $I_m = 3$, and $\epsilon = 3 \times 10^{-2}$. The initial characteristic width of the dark stripe is a couple of times larger than that of the solitary solution (3). As it propagates, the main wide beam experiences self-defocusing. The dark stripe in the center first undergoes self-focusing [2(b) and 2(c)]. Figures 2(b)–2(f) also show some amount of radiative decay with radiated waves seen as dark stripes on a brighter background that originate near the center of the beam and move outward. At larger propagation distances [2(d) and 2(e)], the development of the snake instability results in the periodic bending of the dark channel along the initially homogeneous

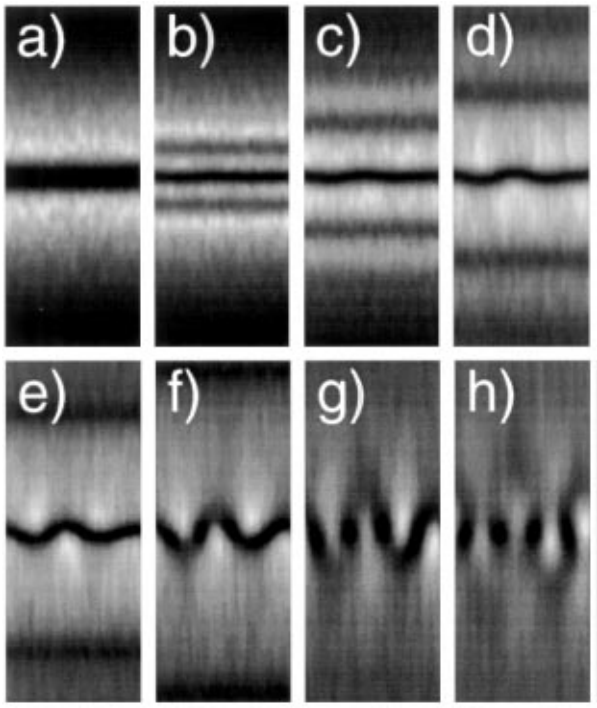

FIG. 2. Evolution of a narrow dark stripe for the longitudinal propagation distance $x = 0$ (a), 5 (b), 10 (c), 15 (d), 20 (e), 25 (f), 30 (g), and 35 (h).

coordinate y. At the same time the continuous line of zeros of the field breaks down into a set of optical vortices or wave front dislocations that become more and more pronounced [2(f)–2(h)]. These dislocations are visualized in Fig. 3 by plotting the product of the real and the imaginary parts of the electromagnetic field for the conditions of 2(g). Dark intertwined lines correspond to zeros of either real or imaginary part, the points of their intersection are zeros of the total field. Figure 3 zooms in on the central part of the beam in Fig. 2 along the z coordinate.

Numerical analysis of the spatial dynamics of beams with a wide embedded dark stripe shows that it cannot exist as a single intensity dip and breaks down into a series of narrower dark stripes. Each of those develops subsequently according to a scenario close to the evolution of the narrow stripe discussed above and shown in Fig. 2.

In the experimental setup shown in Fig. 4 a 10 mW beam from a He-Ne laser ($\lambda = 0.6328\ \mu$m) was focused in the horizontal plane with a pair of cylindrical lenses. The vertical size of the beam remained unchanged and equal to about 2 mm. The beam was directed into a photorefractive crystal placed after the beam waist. The crystal $\hat{c}$ axis was oriented parallel to the z axis to take advantage of the largest component r_{33} of the electro-optic tensor of SBN. A variable dc voltage was applied along the $\hat{c}$ axis to control the value of nonlinear coupling, and the effective dark intensity was varied by illuminating the crystal from above with incoherent white light. Images of

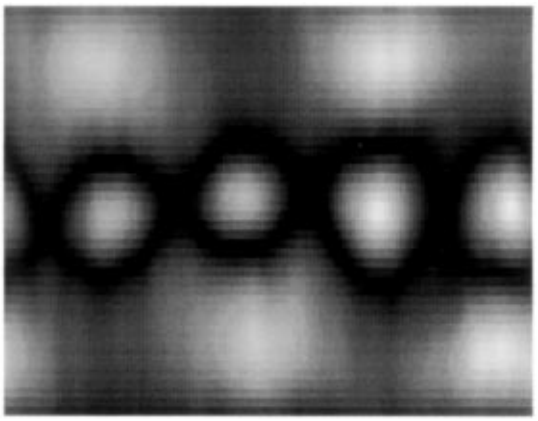

FIG. 3. The product of the real and imaginary parts of the field for Fig. 2(g) ($x = 30$).

the beam at the input and output faces of the crystal were recorded with a charge coupled device camera.

To create a dark stripe parallel to the y axis a glass plate was introduced in half of the beam before the system of two cylindrical lenses. Interference of the reference beam with the light passed through the crystal was used to adjust the tilt of the glass plate to ensure a phase shift of aproximately $2\pi n + 180°$ between the two halves of the main beam passing through the crystal. The same arrangement was used to visualize zeros of the electromagnetic fields generated as the result of decay of the dark stripe (see [12]).

The experimental results presented in Fig. 5 show the steady state intensity profiles of the output beam for different values of the applied voltage (different values of the nonlinearity) and a fixed level of incoherent illumination several times weaker than the initial beam intensity. The vertical size of each picture in Fig. 5 is about 200 μm. Figure 5(a) shows the diffractive spreading of the dark stripe embedded in the beam and the beam itself for zero applied voltage (zero nonlinearity). As the nonlinearity increases the main beam experiences

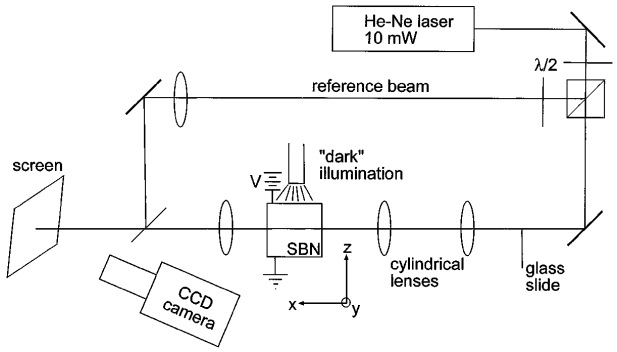

FIG. 4. The experimental setup. The photorefractive crystal of SBN:60, doped with 0.002% by weight Ce, measured $10 \times 6 \times 9$ mm along (x, y, z).

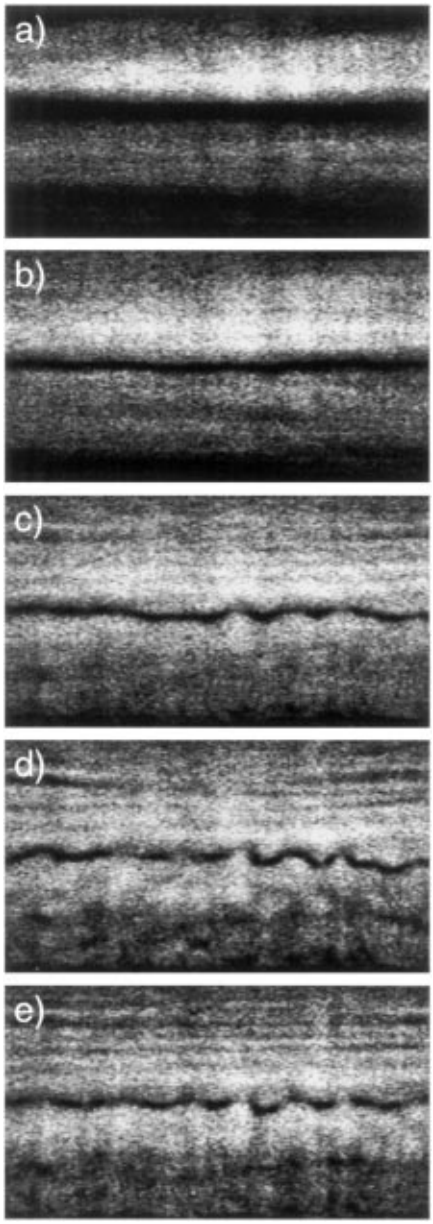

FIG. 5. Intensity distribution of the output field for externally applied voltage equal to (a) 0 V, (b) 400 V, (c) 990 V, (d) 1250 V, and (e) 1410 V.

self-defocusing and the dark stripe starts to self-focus [5(b)]. Further increase in the nonlinearity results in the appearance of characteristic snake distortions on the dark stripe due to the transverse modulation instability [5(c)]. For still larger nonlinearities the initially continuous dark stripe breaks down into a series of isolated zeros of the electromagnetic field, as is seen in 5(d) and 5(e). The existence of the zeros (optical vortices or wave front dislocations [15]) was confirmed experimentally by interferometric measurements. The spacing of the zeros seen in Fig. 5(e) is about 40 μm, which corresponds, using the measured experimental parameters, to $k_y \sim 1$ in Fig. 1. We have also shown experimentally that a wider dark stripe decays by the formation of multiple narrower self-focused dark filaments that subsequently start snaking and decay into a series of vortices.

The authors acknowledge the help of A. Hagen. A.A.Z. acknowledges the support of NSF Grant PHY90-12244 and the Optoelectronics Computing Center, an NSF Engineering Research Center. The work at Risø was supported by the Danish Natural Science Research Council.

*Permanent address: Institute for Problems in Mechanics, Russian Academy of Sciences, Prospekt Vernadskogo 101, Moscow, 117526 Russia.wa

[1] V. E. Zakharov and A. B. Shabat, Zh. Eksp. Teor. Fiz. **64**, 1627 (1973) [Sov. Phys. JETP **37**, 823 (1973)].
[2] V. E. Zakharov and A. M. Rubenchik, Zh. Eksp. Teor. Fiz. **65**, 997 (1973) [Sov. Phys. JETP **38**, 494 (1974)].
[3] E. A. Kuznetsov and S. K. Turitsyn, Zh. Eksp. Teor. Fiz. **94**, 119 (1988) [Sov. Phys. JETP **67**, 1583 (1988)].
[4] V. Tikhonenko, J. Christou, and B. Luther-Davies, J. Opt. Soc. Am. B **12**, 2046 (1995).
[5] C. T. Law and G. A. Swartzlander Jr., Opt. Lett. **18**, 586 (1993).
[6] G. S. McDonald, K. S. Syed, and W. J. Firth, Opt. Commun. **95**, 281 (1993).
[7] G. R. Allan *et al.*, Opt. Lett. **16**, 156 (1991).
[8] G. A. Swartzlander, Jr., *et al.*, Phys. Rev. Lett. **66**, 1583 (1991).
[9] G. A. Swartzlander, Jr., and C. T. Law, Phys. Rev. Lett. **69**, 2503 (1992).
[10] M. D. Iturbe Castillo *et al.*, Opt. Commun. **118**, 515 (1995).
[11] M. Taya *et al.*, Phys. Rev. A **52**, 3095 (1995).
[12] N. B. Baranova *et al.*, Pis'ma Eksp. Teor. Fiz. **33**, 206 (1981) [JETP Lett. **33**, 195 (1981)].
[13] P. Coullet, L. Gil, and F. Rocca, Opt. Commun. **73**, 403 (1989).
[14] Y. Pomeau and S. Rica, C.R. Acad. Sci. Series II **317**, 1287 (1993).
[15] B. Ya. Zel'dovich, A. V. Mamaev, and V. V. Shkunov, *Speckle-Wave Interactions in Application to Holography and Nonlinear Optics* (CRC Press, Boca Raton, 1995).
[16] A. A. Zozulya and D. Z. Anderson, Phys. Rev. A **51**, 1520 (1995).
[17] G. C. Valley *et al.*, Phys. Rev. A **50**, R4457 (1994); M. Segev *et al.*, Phys. Rev. Lett. **73**, 3211 (1994).